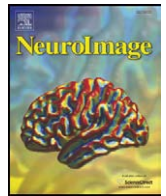


Contents lists available at [ScienceDirect](#)

NeuroImage

journal homepage: www.elsevier.com/locate/ynimg

Technical Note

Functional imaging of the human superior colliculus: An optimised approach

Matthew B. Wall, Robin Walker, Andrew T. Smith*

Department of Psychology, Royal Holloway, University of London, Egham, Surrey, TW20 0EX, UK

ARTICLE INFO

Article history:

Received 8 January 2009

Revised 29 April 2009

Accepted 27 May 2009

Available online xxx

ABSTRACT

Effective functional imaging of the human Superior Colliculus (SC) has often been regarded as difficult because of the small size of the SC and its proximity to sources of pulsatile (cardiac) noise. An optimised approach to functional imaging of the SC with fMRI is presented, based upon the novel finding that visually-induced BOLD responses in the SC are qualitatively different from responses in both cortical (V1) and sub-cortical (LGN) comparison areas. An optimised model with a Haemodynamic Response Function (HRF) which peaks early (4–5 s) and then falls rapidly is shown to be best suited for revealing SC responses, while a model peaking at 6 s and falling more slowly was most sensitive in the two comparison areas. Additionally, a method of correcting for the noise characteristics of fMRI responses proposed recently by de Zwart et al. (de Zwart, J. A., van Gelderen, P., Fukunaga, M., & Duyn, J. H. (2008). Reducing correlated noise in fMRI data. *Magn Reson Med*, 59, 939–945) is modified for use in the SC, and shown to be highly effective at further improving the statistical detectability of responses by modelling out noise. Together these methods represent a significant advance over previous approaches to functional imaging of the human SC. They permit the routine detection of strong SC activity in single subjects at standard spatial resolutions.

© 2009 Elsevier Inc. All rights reserved.

Introduction

The Superior Colliculus (SC) is a small laminar structure located in the dorsal mesencephalon. The superficial layers receive visual inputs from the retina as well as from other visual areas (Robinson and McIlurkin, 1989) and neurons form a topographically coded map of the contralateral visual field. In contrast, neurons in the deeper layers of the superior colliculus receive inputs from cortical and sub-cortical regions subserving sensory and motor functions, including extrastriate visual cortex, multimodal association parietal cortex and prefrontal cortex (Sparks and Hartwich-Young, 1989). These neurons are organised in a two-dimensional motor map coding contralateral eye (saccades) and head movements (Munoz et al., 2000; Sparks and Hartwich-Young, 1989). Neurons located in the rostral region (located beneath the foveal representation) are active during fixation (Munoz and Wurtz, 1993) and those in the caudal region encode shifts of gaze with a specific direction and amplitude. Work on animals has established the SC's role in a diverse range of functions including the straightforward processing of visual information (Goldberg and Wurtz, 1972; Krauzlis, 2004), saccade target selection (Kim and Basso, 2008; McPeck, 2008; Krauzlis et al., 2004), attention (Muller et al., 2005; Ignashchenkova et al., 2004), head movements (Walton et al., 2007, 2008) and even reward processing (Weldon et al., 2007; Ikeda and Hikosaka, 2007).

Functional brain imaging of the human SC has often been regarded as technically challenging (DuBois and Cohen, 2000), because of its small size and its situation next to large blood vessels within and around the brainstem, which produce regular movement as a result of blood pulsation (Poncelet et al., 1992), introducing substantial temporal noise artifacts into acquired data. Some progress in imaging the SC and similarly small brain structures has been enabled by advances in scanning technology. The advent of high-field strength (i.e. ≥ 3 T) MRI systems for human research purposes has enabled the use of higher spatial resolutions while still maintaining a reasonable signal-to-noise ratio. In-plane voxel sizes of approximately 1.5×1.5 mm have been used successfully to obtain visually-related activity in the SC (DuBois and Cohen, 2000; Schneider and Kastner, 2005; Sylvester et al., 2007). Regarding the pulsatile noise artefacts, analysis techniques such as Independent Components Analysis (ICA) may be generally useful in terms of identifying noise sources, however, more specific techniques intended to reduce noise in the SC have also been developed. One method involves cardiac gating (Guimaraes et al., 1998) in which the EPI volume acquisitions are synchronised in real time with the participants' monitored cardiac signal, so that each MRI volume acquisition starts at the same point in the cardiac cycle. This results in a much lower level of cardiac-related temporal noise. Another approach also involves measuring noise sources (cardiac and, optionally, respiratory) at the time of data acquisition, and using that data to define regressors of no interest (nuisance regressors) to allow the noise to be modelled in a multiple regression analysis. Both these approaches appear to be reasonably effective, but both also have disadvantages, a major one being that

* Corresponding author. Fax: +44 1784 434347.
E-mail address: a.t.smith@rhul.ac.uk (A.T. Smith).

they seek to correct only one or two specific sources of noise, whereas noise in fMRI data derives from multiple physiological and technological sources.

A novel method of removing the effects of noise on fMRI data has recently been described by de Zwart et al. (2008). This method is potentially advantageous because it makes no assumptions about the sources of noise in the data, and also attempts to remove *all* noise, whether physiological or technological in origin. It is not well-suited to whole-brain analyses, because it requires comparison voxels of no interest, but it is potentially the most effective extant method for ROI-based analyses. Furthermore, all this method requires is a short 'rest' scan (where the participant is instructed to do nothing); no physiological monitoring is necessary. The method works in several stages. First, the mean time-course of voxels in a ROI (either independently defined, or defined as a result of an initial, standard analysis of the experimental data) during the rest scan is extracted, and that time-course is correlated with the time-course of every voxel in the rest scan, to produce a correlation map. Since there is no task present in the rest scan, fluctuations in the time-courses are assumed to be largely reflective of noise. The correlation map therefore highlights other areas of the brain which share correlated noise characteristics with the primary ROI. Time-courses for all highly correlated voxels are then extracted from the main experimental data and averaged. Based on the assumption that if noise is correlated during rest, it will be correlated during sensory stimulation or task performance, the mean time-course is entered into the analysis as a regressor of no interest, serving to produce a better-fitting overall model and a boost in statistical detection efficiency for the regressors of interest. This method of noise correction has great potential to be applied to areas like the SC, where noise is a particular problem for effective signal detection.

In this paper we present a modified version of the de Zwart et al. (2008) noise-correction method. Instead of using reference voxels scattered around the brain, we define a single reference ROI. In the case of the SC, a convenient reference region is the anterior cerebellum, which is physically close but not directly connected (provided that the ROI does not extend sufficiently posteriorly as to include the cerebellar vermis). The advantage of our approach is that it deals better with the problem that correlation at rest could reflect functional connectivity. If this is the case, some task-related activity will be modelled out by the de Zwart method, along with the noise-related activity. When the reference voxels are scattered around the brain, it is inevitable that some of them will be functionally related and these will impair the efficiency of the correction. Choosing a single reference ROI that is correlated at rest but is thought to have little or no functional relation to the primary ROI avoids this problem.

A second topic of interest was to investigate whether detection sensitivity in the SC can be improved by optimisation of the statistical model used for the analysis – the canonical Haemodynamic Response Function (HRF). Both the amplitude and shape of the HRF have been found to vary significantly across subjects, and across different brain areas (Handwerker et al., 2004; Aguirre et al., 1998), and also within particular patient groups (Bonakdarpour et al., 2007). Investigations of the variability of the BOLD response across the brain have confined themselves to cortical brain areas, with none (to our knowledge) examining the SC or indeed any other sub-cortical structure. If the response in the SC differs substantially from cortical areas, analysis with the canonical HRF as a model will be severely compromised. It is notable that one recent investigation of the SC (Schneider and Kastner, 2005) which did not employ any correction for cardiac noise, also used a somewhat non-standard analysis method (Fourier analysis) which makes few assumptions about the precise shape or timing of the haemodynamic response. By applying a set of systematically varying models to the data, we show that the standard statistical model of the Haemodynamic Response Function (HRF) is inappropriate for the SC, and have developed a more optimal model.

Overall, the purpose of the analyses presented here is to outline and validate an approach to functional imaging of the SC, optimised by the use of two innovative methods, which enables statistically robust responses to be obtained in a single-subject, ROI-based design.

General methods

Participants

Six female undergraduate student volunteers aged 18–22 provided the data for the investigation. All had normal, or corrected-to-normal vision and were screened according to standard MRI exclusion criteria. They were paid for their time. The six data sets were selected at random from a set of sixteen participants who had taken part in a larger study (Smith et al., 2009) which also included additional stimulus conditions to those described below.

Data acquisition

MRI images were obtained with a 3-Tesla Siemens Magnetom Trio scanner and a standard Siemens 8-channel array head coil. Anatomical (T1-weighted) images were obtained at the start of each scanning session (MP-RAGE, 160 axial slices, in-plane resolution 256×256, 1 mm isotropic voxels, TR = 1830 ms, TE = 4.43 ms, flip angle = 11°, bandwidth = 130 Hz/pixel). This was followed by six functional scanning runs. The functional data were acquired with a gradient echo, echoplanar sequence (TR = 1500 ms, 17 contiguous axial slices centred on the thalamus, interleaved acquisition order, 3 mm isotropic voxels, FOV = 192 × 192 mm, flip angle = 80°, TE = 36 ms, bandwidth = 1202 Hz/pixel). Each scan consisted of 190 acquisition volumes and lasted 4 min 45 s. There was also a final (seventh) scan which was identical to the others in every way, except that no stimuli were presented and participants were instructed simply to relax.

Stimuli and design

Visual stimuli were generated by a computer-controlled LCD projector, back-projected onto a screen mounted into the rear of the scanner bore, and viewed through a mirror mounted on the head coil.

A central fixation point was present continuously. Stimuli were presented at an eccentricity of 9 deg to either the right or left of fixation. Each consisted of a large, circular patch (12 deg diam) of 150 moving white dots on a dark background. Each dot subtended 0.5 deg and moved at a speed of 12 deg/sec. Local motion directions were controlled so as to create a global pattern of optic flow. A proportion of the dots (typically 40%) had random directions. The stimulus was based on that of Morrone et al. (2000), in which optic flow varies over time, smoothly changing between expansion/contraction and rotation, via intermediate spiral motions. This stimulus was chosen because of its ability to elicit responses in another thalamic nucleus (the inferior pulvinar, see Cotton and Smith, 2007) which was the main focus of the study from which the current data are drawn. It serves here simply as a general-purpose visual stimulus that should elicit visual responses in the SC. The use of separate trials with the motion stimulus on the left and right allows separation of contralateral and ipsilateral responses.

Each stimulus was presented for 3 s and formed one trial of an event-related design. Participants were required to report the direction of a small change in brightness of the fixation spot that occurred midway through the trial. This task was to ensure that the participants' fixation and attention remained on the fixation spot throughout the trial. The difficulty of this task (magnitude of change) was set so that participants scored approximately 75% correct. Responses were collected via a MRI-compatible response box.

Between trials, the screen was blank apart from the fixation spot. The inter-trial interval (ITI) was varied according to a Poisson

distribution (Hagberg et al., 2001) with an average ITI of 6 s. There were in fact four trial types in the experiment, two of which are described above (left and right stimulus presentation), and a further two which involved the presentation of bilateral stimuli and an attention-to-motion task. All the data and analyses presented here use only the trials which involved a single stimulus presentation in one visual hemifield. There were 8 trials of each type in each of the six scanning runs, to give 48 occurrences of each trial type across a whole scanning session. The order of trials was determined such that each trial type was preceded equally often by each trial type, including itself.

Data analysis

All pre-processing and analyses were performed with BrainVoyager QX, (version 1.9; Brain Innovation, Inc, The Netherlands). Functional data were pre-processed to correct for head-motion and slice-timing, and filtered with a temporal high-pass filter of 0.014 Hz. No spatial smoothing was performed on the functional data. Correction for the effects of serial autocorrelations (which we regard as essential in single-subject analyses, see Smith, Singh and Balsters et al, 2007) was applied using the AR(1) method.

ROI definition

This investigation takes a single-subject approach to examining SC responses, using Region Of Interest (ROI) General Linear Models (GLMs), which are more sensitive than whole-brain analyses because they reduce the multiple-comparisons problem. ROIs therefore had to be defined for each participant. Separate left and right SC ROIs were defined anatomically with reference to a brain atlas (Duvernoy, 1991). The SC (unlike many cortical areas) is anatomically well-defined, and clearly visible on a standard anatomical MRI image, which makes it suitable for an anatomical ROI definition. Additional ROIs were also required for comparison to responses in the SC. These were the Lateral Geniculate Nucleus (LGN), which provides a visually responsive sub-cortical comparison, and the primary visual cortex. These two areas were functionally defined for each subject, based on the results of a standard analysis (see below), and a contrast which subtracted left visual field stimuli from right stimuli. With an uncorrected threshold of $p < 0.001$ this revealed, in every participant, a cluster of activation in the left LGN and another in primary visual cortex, and separate clusters of activity in the right LGN and visual cortex that appeared as negative following the subtraction, reflecting the contralateral response mappings of early portions of the visual system. LGN ROIs were defined based on these activation clusters. Primary visual cortex ROIs were defined as the part of the large activation cluster in the visual cortex which lay in and around the calcarine sulcus. This tended to be restricted to a region about half way along the sulcus, reflecting the stimulus eccentricity. The ROI can be assumed to consist mainly of area V1, together with some voxels in area V2. For the purposes of the present study and as a comparison site for the SC, the exact constitution is unimportant, and this ROI will hereafter be referred to simply as 'V1'. See Fig. 1 (upper panel) for example ROIs.

Analyses using custom haemodynamic response functions

Exploratory analyses which involved examining time-courses of responses in the SC, and used a variety of custom regressors in order to model SC responses, indicated that the SC may have a different response profile compared to other sub-cortical and cortical brain areas. It was therefore decided to investigate whether the standard Haemodynamic Response Function (HRF) is the optimal model for responses in the SC. The standard HRF is a synthetic function produced by combining two gamma functions (Friston et al., 1998; Handwerker et al., 2004), and is implemented in many popular software packages

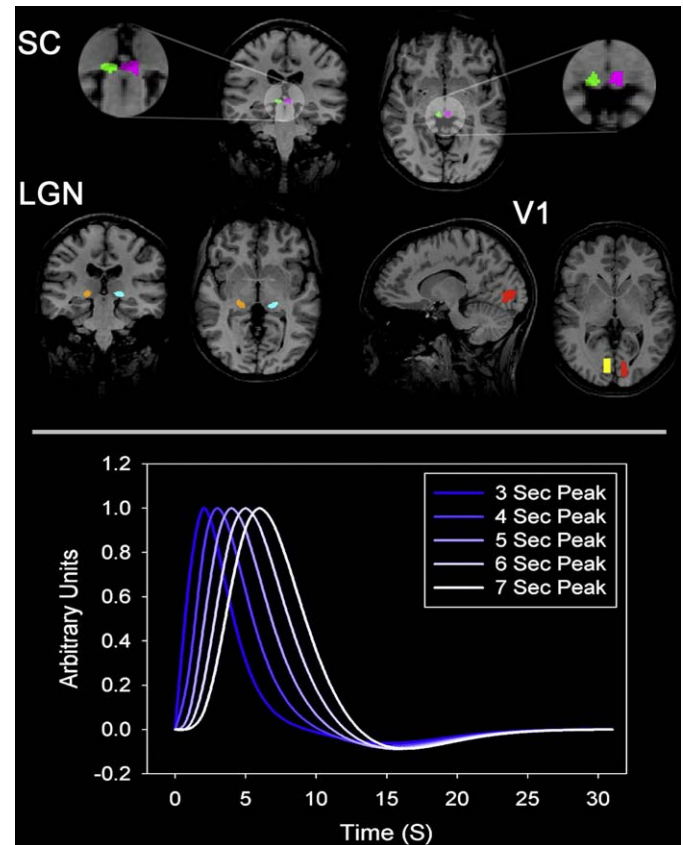


Fig. 1. Upper panel: ROIs from representative participants. Pink = SC right, green = SC left, cyan = LGN right, orange = LGN left, red = V1 right, yellow = V1 left. Brain images in neurological (left of the image = participant's left) format. Lower panel: custom HRFs used in the analyses. The time-to-peak of the function was varied between 3 and 7 s. The standard HRFs used in most neuroimaging investigations peak at 5–6 s.

(with minor variations) for the analysis of functional imaging data. This function is then typically convolved with a binary function specifying the event timings, in order to produce the final regressors for inclusion in a model for analysis of a data set. BrainVoyager QX enables the creation of custom HRFs by varying the parameters of the gamma functions. In this investigation, a set of five synthetic HRFs was created. These differed in terms of time-to-peak, which varied between 3 and 7 s with a corresponding change in the width of the function (see Fig. 1, lower panel).

These custom functions were convolved with a function derived from stimulus onset and offset vectors for each trial type, in the standard manner, in order to produce a set of five models. As well as modelling the two stimulus conditions presented here, each model also included regressors related to the two additional stimulus conditions referred to above, which for the purposes of the present results can be considered as regressors-of-no-interest. Each model also included regressors derived from the participants' motion correction parameters as regressors-of-no-interest.

The first analysis conducted used the standard (6 s peak) HRF provided by BrainVoyager, and a whole-brain contrast was derived which subtracted left from right visual field stimuli. Such an analysis revealed robust differential activation clusters throughout the visual cortex, and was also sufficient to reveal contralateral LGN activity in all participants, although not always the SC. This contrast served as the basis for defining the LGN and V1 ROIs (see 'ROI definition' above). A set of ROI GLM analyses were then conducted, using data from the functionally-defined V1 and LGN, and the anatomically defined SC, ROIs. Each ROI GLM used a different set of regressors, defined by convolving the stimulus time functions with each of the set of custom HRFs described above. Beta estimates were derived for

each condition, within each analysis and each ROI. The results are shown in Fig. 2.

All three areas show clear contralateral responses to the left and right visual stimuli. In V1 and the LGN, the standard 6-second peak HRF appears to be optimal for the detection of such responses. However, the SC shows a different pattern, such that signal detection is most efficient with HRFs which peak at 4 and 5 s, and is in fact highly inefficient with the standard model. This surprising finding suggests that visually-induced BOLD responses in the SC have a different temporal profile from responses in cortical visual areas, and also from the sub-cortical (and anatomically more proximal) LGN. It suggests that the SC response peaks early and also falls rapidly, giving a negative correlation with the 7 s model, not seen in the LGN or V1, because the response is already falling during the rising portion of the model (compare the 4 s and 7 s functions in Fig. 1).

The ipsilateral responses mirror the contralateral responses, but are much smaller. They are smallest (essentially absent) in V1 and largest in SC. The ROI data were analysed using a 5 (HRF-peak; 3–7 s) × 3 (ROI; SC, V1 and LGN) × 2 (Ipsilateral vs. Contralateral) ANOVA, which returned highly significant results. All three main

effects, the three orthogonal 2-way interactions, and the 3-way interaction were significant ($F > 15$, $p < 0.01$ in all cases).

In order to directly assess the shapes of the responses in the different brain regions, event-related averaged time-courses were extracted from the three ROIs and averaged across participants. For the purposes of presentation clarity and to reduce noise, contralateral and ipsilateral responses were each averaged across hemispheres (see Fig. 3, panels A and B). Since the design of this experiment was event-related and incorporated relatively short ITIs, a large degree of interference from previous and subsequent trials is evident in the time-courses, despite the use of a variable ITI. For instance, a trough can be seen in the responses prior to the rising stimulus-related response, which represents the falling portion of the BOLD response related to the previous trial. Additionally, a second peak can be seen at around 13 s, which represents the response to the next trial, although the amplitude of this peak is reduced by smoothing due to the variability of the ITI. In order to isolate the stimulus-related response more effectively, the averaged ipsilateral time-course was subtracted from the averaged contralateral time-course. Because the trial presentation order was fully counterbalanced, the contralateral and ipsilateral curves should contain the same contributions from

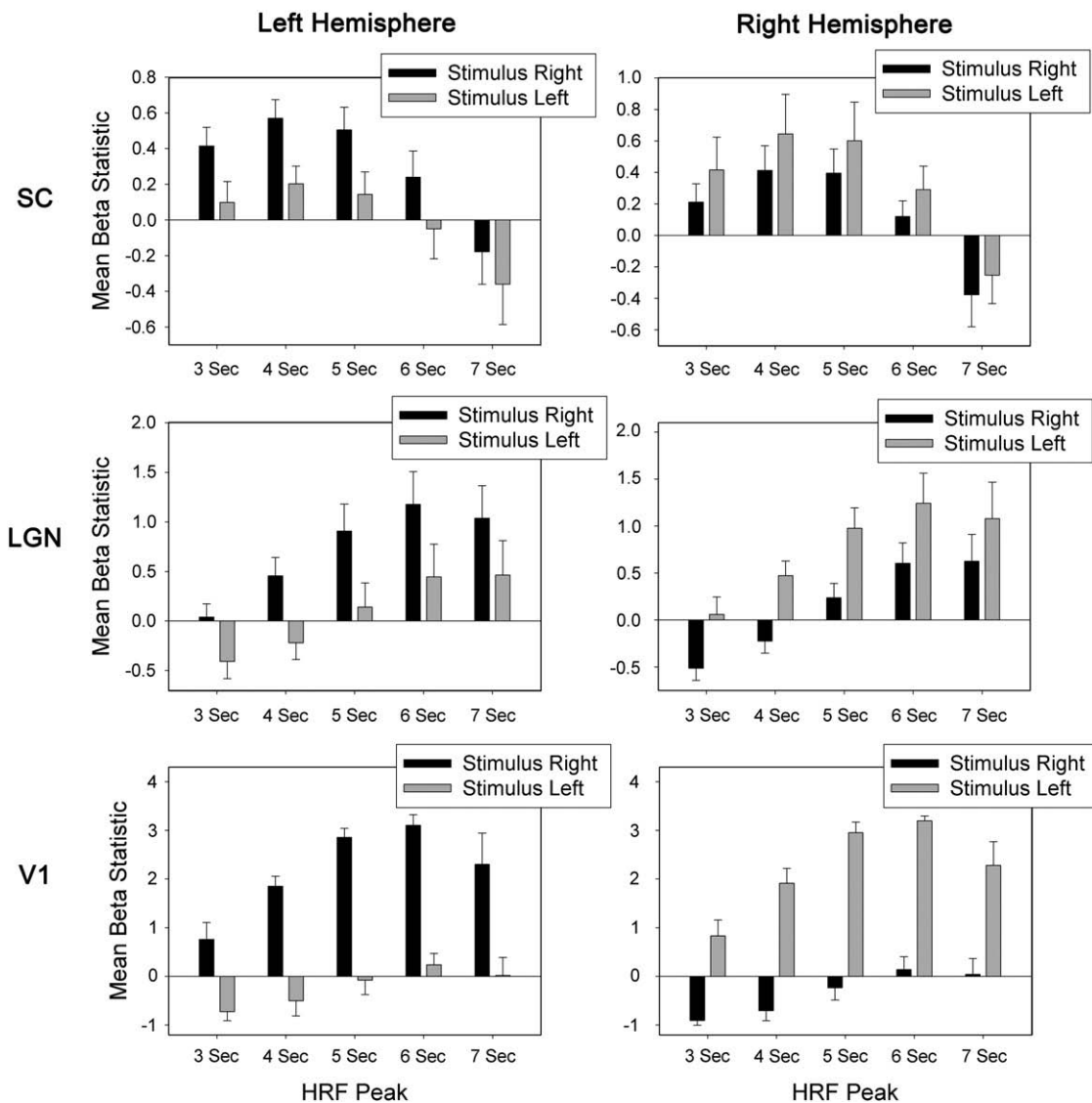


Fig. 2. Results from the analyses using custom-shaped HRFs. Results from the left hemisphere in the left column, and right hemisphere in the right. Top row shows data from the SC, middle from the LGN and bottom from V1. Histograms show mean beta statistics averaged across subjects, error bars represent standard errors of the mean. The standard (6 s peak) HRF is optimal for LGN and V1, but is sub-optimal for the SC.

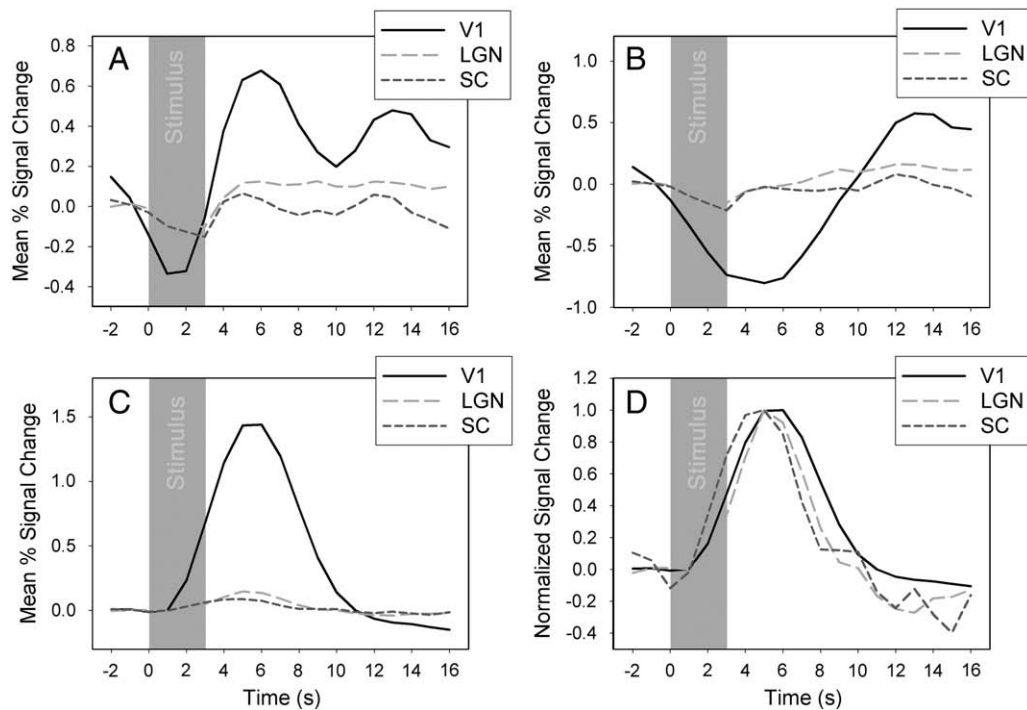


Fig. 3. Mean (averaged across participants) time-courses of responses in V1, LGN and SC. The grey bar represents stimulus presentation. Panel A: responses from contralateral stimuli/hemispheres i.e. right hemisphere on left-stimulus trials and left hemisphere on right-stimulus trials. Panel B: responses from ipsilateral stimuli/hemispheres i.e. left hemisphere on left-stimulus trials and right hemisphere on right-stimulus trials. Panel C: The result of subtracting the curves in panel B from those in panel A, thereby isolating the stimulus-related response. Panel D: Normalised version of the data in panel C. This plot reveals a phase-difference of approximately 1 s between responses in the SC and V1/LGN.

adjacent trials. Subtracting ipsilateral (which contains only a small response) from contralateral therefore isolates the response to the trial type in question. Fig. 3, panel C shows the result of this subtraction; a large response in V1 and much smaller responses in LGN and SC. In order to visualise the differences between these curves more clearly, the three curves were normalised by dividing every data point by the maximum value for that curve (Fig. 3, panel D).

These time-courses reveal a systematic difference between responses in the SC and responses in the LGN and V1, such that the BOLD response both rises and decays more quickly. Compared to V1, the difference is slightly less than a second in the rising phase of the response, and somewhat more than a second in the falling portion. This response profile is therefore consonant with the results of the statistical analyses described above, and accounts for why a modelled HRF with a peak of 4 or 5 s produces optimal results, and why the standard HRF (6 s peak) is sub-optimal. The LGN response also seems to fall earlier than in V1, but this is not reflected in Fig. 2 and so may not be reliable. The rising portion is very similar in LGN and V1.

Analyses with noise-reduction regressors

As noted in the introduction, functional imaging of the SC is thought to be particularly susceptible to physiological noise artifacts because of its proximity to several large blood vessels (Poncellet et al., 1992). Various methods of mitigating the effects of this pulsatile noise problem have been proposed, however each of these methods also has disadvantages which serve to introduce other sources of noise, or reduce statistical sensitivity in other ways. A novel method has recently been proposed by de Zwart et al. (2008) which has important theoretical advantages over previous methods (see Introduction).

In the original description of this method, de Zwart et al. (2008) used all the voxels in the brain which correlated with the primary ROI above a certain threshold, at rest, to produce the secondary ROI.

Although impressive improvements in sensitivity were obtained, this approach may nonetheless be sub-optimal. Some voxels will be correlated because they are functionally connected and share neural noise (or signals), rather than because they share physiological noise. This is particularly true in visual paradigms, since a large proportion of the brain shows responses to visual stimuli. If a visually responsive area is included in the secondary ROI, and its time-course extracted from the main experimental data to be used as a nuisance regressor, then not only noise, but also a significant amount of signal is likely to

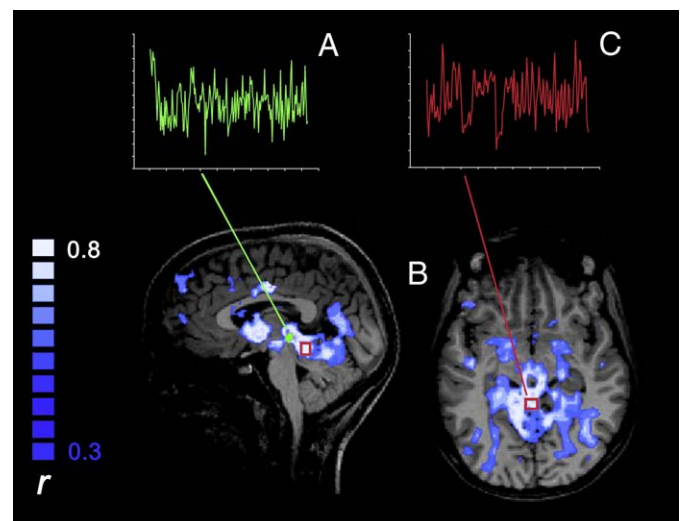


Fig. 4. Noise-correction method. (A) Mean rest-scan time-course of voxels in the SC ROI of one participant (highlighted in green on the sagittal slice in B). (B) This time-course is correlated with all voxels in the rest scan to produce a correlation map, visualised here as a functional overlay in a blue-to-white scale. The correlation map is used to identify a correlated area in the anterior cerebellum, (highlighted on both brain slices as a red outline). (C) Mean time-course from the main experimental data for this ROI, to be entered into the analysis as a regressor of no interest.

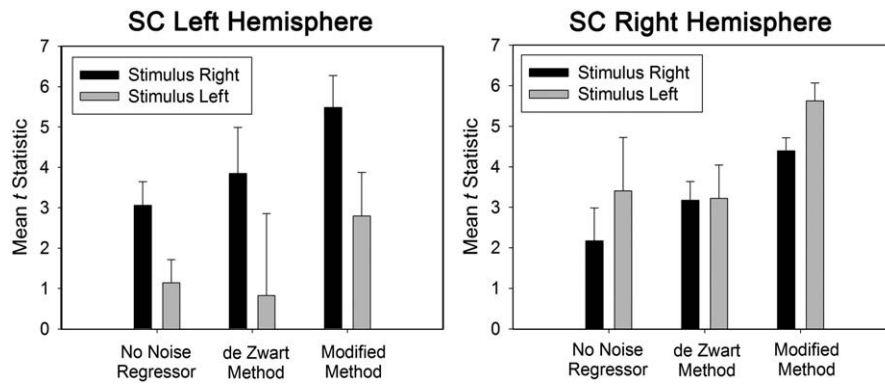


Fig. 5. Mean t -values from ROI GLM analyses (with a 4-second peak HRF) of the SC with and without the noise regressors. Averages are across participants, as well as across voxels in each ROI, and error bars represent the standard error of the mean based on the number of participants. Inclusion of the noise regressor in the model is highly effective at increasing the statistical reliability of results related to the regressors of interest, leading to an average increase in t -values of approximately 2.

be modelled by the regressor, and thus effects associated with the regressors of interest will be weakened.

For this reason, a modified version of the de Zwart et al. (2008) method was developed. This involved producing a correlation map based on a single primary ROI produced by concatenating the left and right SC ROIs, and selecting a single secondary area in the anterior cerebellum. This region was chosen because it is anatomically very close to the SC, has a similar blood supply and therefore may have a similar cardiac noise profile (in form if not amplitude), yet is functionally unrelated, playing no (major) role in visual processing. Care was taken to exclude the vermis, since this part of the cerebellum is known to receive signals related to vision and eye movements (Suzuki et al., 1981). Examination of the correlation maps showed that the time-courses of the anterior cerebellar region did indeed correlate highly with the SC during the rest scan in all participants. An example correlation map, with ROIs marked, is shown in Fig. 4.

Analyses using the optimal model for obtaining SC responses from the previous section (4-second peak HRF) were repeated for each subject, including noise regressors derived from the anterior cerebellum. The effectiveness of the noise reduction method was assessed in terms of its impact on the mean t -values obtained for voxels in the anatomically defined SC ROI and the results are shown in these terms in Fig. 5. Statistical analysis of these values revealed that inclusion of the noise regressor made a significant difference to stimulus-related t -values; $t(11) = 2.35$, $p < 0.05$ (ipsilateral conditions) and $t(11) = 3.84$, $p < 0.005$ (contralateral conditions).

Clearly, inclusion of the noise regressor makes a substantial difference to the statistical reliability of the results, increasing average t -values by approximately 2 in each case. This is comparable to the statistical increase described by de Zwart et al. (2008). Inclusion of the noise regressors also led to an increase in the average overall goodness-of-fit of the models from $R = 0.22$ without the noise regressor, to $R = 0.56$ with the noise regressor. Individual p values for each subject and condition were all below 0.0001 with the inclusion of the noise regressor. This method of noise correction is therefore not only attractive on both theoretical and pragmatic grounds, but is also empirically highly effective at increasing statistical reliability and signal detection of SC responses.

Discussion

The data presented here demonstrate firstly that standard HRF models are sub-optimal for investigations of the human superior colliculus; instead a HRF which peaks somewhat earlier (4 to 5 s) is much more effective than a standard HRF in detecting activation. Secondly, a modified version of a recently described noise-correction method for fMRI (de Zwart et al., 2008) has been developed for the SC and been shown to be highly effective. The combination of these two

methods has produced a set of highly robust statistical results, using a ROI-based single-subject design, repeated on several subjects.

Schneider and Kastner (2005) note that despite the existence of a relatively large number of studies examining visual responses in the human brain, only a few studies have reported activations in the SC. Their explanation is that most studies have used large voxels (i.e. $> 3 \times 3 \times 3$ mm) and that higher spatial resolutions are required to reveal SC activity. While high spatial resolution is undoubtedly useful when imaging small structures like the SC, there is a severe cost in terms of SNR. The present study uses the currently standard resolution (3 mm isotropic voxels) to produce a set of highly robust results. An alternative explanation for the paucity of reported results concerning the SC in the literature is that BOLD responses in the SC have a different form from other commonly investigated brain areas, are particularly prone to physiological (particularly cardiac) noise, and are consequently not easily revealed by standard analysis methods. While the magnitude of the difference in the BOLD response may appear small (approximately 1 s in terms of time-to-peak, see Fig. 3), it has a large effect on the statistical detectability of responses when a standard model is used. A severe effect of a 1 s misalignment of the model with the response in producing false negatives has previously been noted by Handwerker et al. (2004).

Several established methods exist for dealing with BOLD response functions that deviate from standard or ‘canonical’ models. One is the inclusion of two or more HRF regressors based on different impulse responses, such as those shown in Fig. 1, so that between them they capture the signal despite unknown variations in its timing. A popular approach is to use a canonical model together with its derivative; this approach should be adequate for modelling activity in the SC. Another approach is to use a Fourier basis set. This will flexibly model unusual BOLD responses, but carries a risk of ‘over-fitting’ the time-course i.e. modelling noise as well as signal and so erroneously interpreting some of the noise as signal. A third approach is to use finite impulse response (FIR) methods, which essentially consider each point in the time-course independently, removing the need to make assumptions about the temporal structure of the BOLD response, at the cost of some loss of statistical sensitivity. Finally, the use of independent components analysis (ICA) also avoids any assumptions about the form of the response. These methods have all been discussed in detail elsewhere.

Thus, our finding of fast BOLD responses in the SC can be accommodated during data analysis using any of several methods. However, the reality is that some (perhaps many) researchers do not use any of the available methods routinely and this may have contributed to past difficulties in imaging the SC. To capture BOLD responses in the SC successfully, it is necessary either to use one of these methods or else to use a single model that peaks at 4–5 s.

Reasons for the difference in time-course

The question of why responses in the SC differ both from cortical (V1) and other sub-cortical (LGN) areas remains open. Several previous investigations have focussed on examining the shape and variability of the BOLD response in some detail. Aguirre et al. (1998) used a region in the central sulcus, and found significant variability across participants, with much less variability within subjects. Handwerker et al. (2004) reported greater variability across participants than across different brain areas in the shape of the BOLD response, however their reported correlations in the time-to-peak of the response across brain areas, while significant, are far from perfect (ranging from $r=0.39$ to 0.65). Birn, Saad and Bandettini (2001) examined non-linear aspects of the BOLD response at short stimulus durations in both motor and visual cortices, finding considerable variability between different voxels within each area. De Zwart et al. (2005) found variations within the cortex that correlated with proximity to large veins. However, none of these human studies has explicitly compared cortical to sub-cortical regions such as the SC.

One possibility to be considered in relation to our experimental design is that the apparent difference in the BOLD time-course in the SC and V1 might arise from a more transient neural responses in the SC, which may lead to a correspondingly short time-to-peak and shorter-lived BOLD response. During data analysis, we always convolved our HRFs with the 3 s stimulus time-courses, so the resulting models may have been less appropriate for SC than for LGN and V1. One possible effect of this is that the greatest correlation in SC might be found with a model that peaks earlier than the actual BOLD peak, giving a false impression of a short time-to-peak when in fact the BOLD impulse response function might be the same as in V1. Two pieces of evidence militate against this interpretation. Firstly, the time-course data presented in Fig. 3 suggest that the duration of the BOLD response in the SC is very similar to that in the LGN and V1. Secondly, we have performed additional analyses that make such an explanation unlikely. We re-analyzed the data using a more transient model in which stimulus duration was specified as 100 ms (rather than 3 s), to model transient neural responses to stimulus onset rather than sustained responses. If SC responses have a transient form then this model should provide a better fit and hence yield bigger effect sizes. In addition, any apparent shift in the peak due to the model having an inappropriate shape should vanish. The results (presented in full in supplementary Figure 1) show a very similar overall pattern to those shown in Fig. 2, with a strong tendency for the HRFs with a shorter peak to better model responses in the SC, compared to V1 and LGN. The main difference was that the estimated effect sizes are weaker (in terms of % signal change) in all three areas, including SC, presumably because the model being used is now less appropriate for the stimulus presentation regime. While these results suggest that the SC responses are indeed similar in duration to those in LGN and V1, it should be noted that this is not a definitive test, and further work is required before a firm explanation for the observed differences in time-to-peak can be advanced.

One recent fMRI study in rats (Pawela et al., 2008) is consistent with the present data in identifying a slightly faster onset time of the BOLD response in the SC, compared to cortical areas. Explanations for why the SC appears to show a faster BOLD response may be couched in terms of differences in the surrounding vasculature, or perhaps the specific metabolic characteristics of SC cells. Liu et al. (2006) recently showed an earlier time-to-peak of the BOLD response in early visual areas when using stimuli optimised for parvocellular (*P*) pathways, compared to magnocellular (*M*) optimised stimuli. These authors' interpretation is that the difference reflects variations in the rates of aerobic metabolism in *M* and *P* cells, such that *P* cells produce less

deoxygenated haemoglobin (Hb), which allows the detectable ratio between oxygenated and deoxygenated Hb (Hbo/Hb; the basis of the BOLD response) to be reached faster. Applying such an explanation to the present data is necessarily somewhat speculative, and clearly more work is required both to establish whether the reported response profile is unique to the SC or is also evident elsewhere, and to understand its physiological origin.

Correction for spatially correlated noise

The additional analyses using a modified version of the de Zwart et al. (2008) noise-correction method have proven to be highly effective in correcting for pulsatile and other noise present in SC responses. This method is superior to other previously proposed noise reduction methods in that it makes no assumptions regarding the source of noise, and theoretically can correct for noise arising from any source. The method obviates the need for cardiac triggering of scanner volume acquisitions (Guimaraes et al., 1998), which avoids the introduction of another noise source. In addition, it requires no recording of physiological functions (cardiac and/or respiration cycles) during scanning; all that is needed is a short additional rest scan. In sum, this approach has significant advantages over previously proposed methods of correcting for temporal noise in the SC.

The main potential disadvantage is perhaps that only that portion of the noise that is spatially correlated with a remote reference region can be removed. However, we were able to find many voxels with correlations in the region of 0.6 (which represents a p value of approximately 2.5×10^{-19}), which is sufficient to provide a very worthwhile degree of correction. To estimate the upper limit of the noise that it might be possible to remove, we cross-correlated the time-courses of a number of functional voxels within the SC, at rest, in each participant. The mean correlation coefficient was 0.46, indicating that although there is significant spatial correlation, a substantial portion of the noise is uncorrelated.

Another potential problem with the method is that the correlation with the reference ROI at rest may reflect functional connectivity (e.g. Biswal et al, 1995) rather than correlated non-neural noise. If so, the stimulus-related signal may also be correlated and some of the signal may be modelled out as noise. However, (i) this would result in a decrease in t rather than an increase, so, at least in our case, the correlation derives primarily from noise not connectivity, and (ii) functional connectivity at rest is mainly associated with low frequencies and we used a temporal high-pass filter when pre-processing our functional data. The modified version of the method we have used here, in which scattered correlated voxels are replaced by a single, carefully chosen reference region, makes it easier to avoid correlations that reflect connectivity.

Conclusion

We have presented a highly optimised approach to functional imaging of the human superior colliculus, based on two advances. Firstly we have found that the SC appears to have a somewhat different BOLD response profile from other visually-responsive cortical and sub-cortical areas. Secondly, we have modified a recently proposed noise-correction method (de Zwart et al., 2008) for the SC, and found it to be highly effective in increasing the statistical detectability of results. With the combination of these two methods, it becomes straightforward to obtain reliable BOLD responses in the superior colliculus, an important sub-cortical structure that is under-researched in humans. The few fMRI studies of the human SC have so far been restricted (with the exception of Gitelman et al., 2002) to examining visual functions; these methods may enable study of its important role in goal-directed shifts of gaze and attention. An awareness that the HRF can be different outside the cortex may also

aid the study of the many other sub-cortical structures that have yet to be studied in detail with fMRI.

Appendix A. Supplementary data

Supplementary data associated with this article can be found, in the online version, at doi:10.1016/j.neuroimage.2009.05.094.

References

- Aguirre, G.K., Zarahn, E., D'Esposito, M., 1998. The variability of human, BOLD hemodynamic responses. *NeuroImage* 8, 360–369.
- Bonakdarpour, B., Parrish, T.B., Thompson, C.K., 2007. Hemodynamic response function in patients with stroke-induced aphasia: implications for fMRI data analysis. *NeuroImage* 36, 322–331.
- Birn, R.M., Saad, Z.S., Bandettini, P.A., 2001. Spatial heterogeneity of the nonlinear dynamics in the fMRI BOLD response. *NeuroImage* 14, 817–826.
- Biswal, B., Yetkin, F.Z., Haughton, V.M., Hyde, J.S., 1995. Functional connectivity in the motor cortex of resting human brain using echo-planar MRI. *Magn. Reson. Med.* 34, 537–541.
- Cotton, P.L., Smith, A.T., 2007. Contralateral visual hemifield representations in the human pulvinar nucleus. *J. Neurophysiol.* 98, 1600–1609.
- de Zwart, J.A., Silva, A.C., van Gelderen, P., Kellman, P., Fukunaga, M., Chu, R., Koretsky, A.P., Frank, J.A., Duyn, J.H., 2005. Temporal dynamics of the BOLD fMRI impulse response. *NeuroImage* 24, 667–677.
- de Zwart, J.A., van Gelderen, P., Fukunaga, M., Duyn, J.H., 2008. Reducing correlated noise in fMRI data. *Magn. Reson. Med.* 59, 939–945.
- DuBois, R.M., Cohen, M.S., 2000. Spatiotopic organization in human superior colliculus observed with fMRI. *NeuroImage* 12, 63–70.
- Duvernoy, H.M., 1991. *The Human Brain*. Springer-Verlag, New York.
- Friston, K.J., Fletcher, P., Josephs, O., Holmes, A., Rugg, M.D., Turner, R., 1998. Event-related fMRI: characterizing differential responses. *NeuroImage* 7, 30–40.
- Gitelman, D.R., Parrish, T.B., Friston, K.J., Mesulam, M.M., 2002. Functional anatomy of visual search: regional segregations within the frontal eye fields and effective connectivity of the superior colliculus. *NeuroImage* 15, 970–982.
- Goldberg, M.E., Wurtz, R.H., 1972. Activity of superior colliculus in behaving monkey. I. Visual receptive fields of single neurons. *J. Neurophysiol.* 35, 542–559.
- Guimaraes, A.R., Melcher, J.R., Talavage, T.M., Baker, J.R., Ledden, P., Rosen, B.R., et al., 1998. Imaging subcortical auditory activity in humans. *Hum. Brain Mapp.* 6, 33–41.
- Handwerker, D.A., Ollinger, J.M., D'Esposito, M., 2004. Variation of BOLD hemodynamic responses across subjects and brain regions and their effects on statistical analyses. *NeuroImage* 21, 1639–1651.
- Hagberg, G., Zito, G., Patria, F., Sanes, J., 2001. Improved detection of event-related functional MRI signals using probability functions. *NeuroImage* 14, 1193–1205.
- Ignashchenkova, A., Dicke, P.W., Haarmeier, T., Thier, P., 2004. Neuron-specific contribution of the superior colliculus to overt and covert shifts of attention. *Nat. Neurosci.* 7, 56–64.
- Ikeda, T., Hikosaka, O., 2007. Positive and negative modulation of motor response in primate superior colliculus by reward expectation. *J. Neurophysiol.* 98, 3163–3170.
- Kim, B., Basso, M.A., 2008. Saccade target selection in the superior colliculus: a signal detection theory approach. *J. Neurosci.* 28, 2991–3007.
- Krauzlis, R.J., 2004. Activity of rostral superior colliculus neurons during passive and active viewing of motion. *J. Neurophysiol.* 92, 949–958.
- Krauzlis, R.J., Liston, D., Carello, C.D., 2004. Target selection and the superior colliculus: goals, choices and hypotheses. *Vision Res.* 44, 1445–1451.
- Liu, C.S., Bryan, R.N., Miki, A., Woo, J.H., Liu, G.T., Elliott, M.A., 2006. Magnocellular and parvocellular visual pathways have different blood oxygen level-dependent signal time courses in human primary visual cortex. *AJNR Am. J. Neuroradiol.* 27, 1628–1634.
- McPeck, R.M., 2008. Reversal of a distractor effect on saccade target selection after superior colliculus inactivation. *J. Neurophysiol.* 99, 2694–2702.
- Morrone, M.C., Tosetti, M., Montanaro, D., Fiorentini, A., Cioni, G., Burr, D.C., 2000. A cortical area that responds specifically to optic flow, revealed by fMRI. *Nat. Neurosci.* 3, 1322–1328.
- Muller, J.R., Philiastides, M.G., Newsome, W.T., 2005. Microstimulation of the superior colliculus focuses attention without moving the eyes. *Proc. Natl. Acad. Sci. U. S. A.* 102, 524–529.
- Munoz, D.P., Dorris, M.P., Pare, M., Everling, S., 2000. On your mark, get set: brainstem circuitry underlying saccadic initiation. *Can. J. Physiol. Pharmacol.* 78, 934–944.
- Munoz, D.P., Wurtz, R.H., 1993. Fixation cells in monkey superior colliculus I. Characteristics of cell discharge. *J. Neurophysiol.* 70, 559–575.
- Pawela, C.P., Hudetz, A.G., Ward, B.D., Schulte, M.L., Li, R., Kao, D.S., et al., 2008. Modeling of region-specific fMRI BOLD neurovascular response functions in rat brain reveals residual differences that correlate with the differences in regional evoked potentials. *NeuroImage* 41, 525–534.
- Poncellet, D., Lencki, R., Beaulieu, C., Halle, J.P., Neufeld, R.J., Fournier, A., 1992. Production of alginate beads by emulsification/internal gelation. I. Methodology. *Appl. Microbiol. Biotechnol.* 38, 39–45.
- Robinson, D.L., McGlurkin, J.W., 1989. The visual superior colliculus and pulvinar. In: Wurtz, R.H., Goldberg, M.E. (Eds.), *The Neurobiology of Saccadic Eye Movements*. Elsevier Science Publishers B.V., pp. 337–360.
- Schneider, K.A., Kastner, S., 2005. Visual responses of the human superior colliculus: a high-resolution functional magnetic resonance imaging study. *J. Neurophysiol.* 94, 2491–2503.
- Smith, A.T., Singh, K.D., Balsters, J.H., 2007. A comment on the severity of the effects of non-white noise in fMRI time-series. *NeuroImage* 36, 282–288.
- Smith, A.T., Cotton, P.L., Bruno, A., Moutsiana, C., 2009. Dissociating vision and visual attention in the human pulvinar. *J. Neurophysiol.* 101, 917–925.
- Sparks, D.L., Hartwich-Young, R., 1989. The deep layers of the superior colliculus. In: Wurtz, R.H., Goldberg, M.E. (Eds.), *The Neurobiology of Saccadic Eye Movements*. Elsevier Science Publishers B.V., pp. 213–255.
- Suzuki, D.A., Noda, H., Kase, M., 1981. Visual and pursuit eye-movement related activity in the posterior vermis of monkey cerebellum. *J. Neurophysiol.* 46, 1120–1139.
- Sylvester, R., Josephs, O., Driver, J., Rees, G., 2007. Visual fMRI responses in human superior colliculus show a temporal-nasal asymmetry that is absent in lateral geniculate and visual cortex. *J. Neurophysiol.* 97, 1495–1502.
- Walton, M.M., Bechara, B., Gandhi, N.J., 2007. Role of the primate superior colliculus in the control of head movements. *J. Neurophysiol.* 98, 2022–2037.
- Walton, M.M., Bechara, B., Gandhi, N.J., 2008. Effect of reversible inactivation of superior colliculus on head movements. *J. Neurophysiol.* 99, 2479–2495.
- Weldon, D.A., DiNieri, J.A., Silver, M.R., Thomas, A.A., Wright, R.E., 2007. Reward-related neuronal activity in the rat superior colliculus. *Behav. Brain Res.* 177, 160–164.